Kinetics and Mechanism for the Metalation of 5,10,15,20-Tetrakis(pentafluorophenyl)porphyrin with Bis(*β*-diketonato)copper(II) Complexes in Supercritical Carbon Dioxide and *n*-Hexane

Yasuhiro Inada,[†] Hideyuki Sato,[‡] Shi-jun Liu,[‡,§] Taichi Horita,[‡] and Shigenobu Funahashi*[,‡]

Research Center for Materials Science, Nagoya University, Chikusa, Nagoya 464-8602, Japan, and Graduate School of Science, Nagoya University, Chikusa, Nagoya 464-8602, Japan

Received: August 12, 2002; In Final Form: December 13, 2002

The copper(II) ion incorporation reactions into 5,10,15,20-tetrakis(pentafluorophenyl)porphyrin (H_2tpfpp) to form the Cu(tpfpp) complex have been kinetically investigated with bis(*β*-diketonato)copper(II) complexes (CuL_2) such as bis(1,1,1,5,5,5-hexafluoropentane-2,4-dionato)copper(II) ($Cu(hfac)_2$), bis(1,1,1-trifluoropentane-2,4-dionato)copper(II) ($Cu(tfac)_2$), bis(2,2,6,6-tetramethylheptane-3,5-dionato)copper(II) ($Cu(hmac)_2$), and bis(pentane-2,4-dionato)copper(II) ($Cu(acac)_2$) in supercritical carbon dioxide ($scCO_2$) using a previously developed stopped-flow instrument and spectrophotometric cell. Saturation dependence was observed for the conditional first-order rate constants (k_{obs}) as a function of the mole fraction of excess CuL_2 (x_{Cu}): $k_{obs} = k_2K_1x_{Cu}/(1 + K_1x_{Cu})$, where K_1 is the preequilibrium constant for the fast outer sphere association between H_2tpfpp and CuL_2 and k_2 is the first-order rate constant for the rate-determining copper(II) ion incorporation into the porphyrin core. Under constant temperature (333 K) and pressure (20.0 MPa), the K_1 values are in the order of $Cu(hfac)_2 < Cu(tfac)_2 < Cu(hmac)_2 < Cu(acac)_2$; this trend has been interpreted by the differences in the solvation energy of the CuL_2 complexes in $scCO_2$ and in the electrostatic repulsion between H_2tpfpp and CuL_2 anticipated in the outer sphere association complex. On the other hand, the k_2 values are in the following order: $Cu(hfac)_2 > Cu(tfac)_2 > Cu(hmac)_2 > Cu(acac)_2$. This order may be explained by the affinity of CuL_2 for the nucleophile of the pyrrolenine nitrogen, the easiness of dissociation of the *β*-diketonate ligand, and the electrostatic repulsion between H_2tpfpp and CuL_2. The thermodynamic and kinetic parameters in $scCO_2$ were obtained as follows: $K_1 = (5.2 \pm 0.1) \times 10^4$ (333 K, 20.0 MPa), $\Delta H_1^\circ = 76 \pm 2$ kJ mol^{-1} (20.0 MPa), $\Delta S_1^\circ = (3.2 \pm 0.7) \times 10^2$ J mol^{-1} K^{-1} (20.0 MPa), $\Delta V_1^\circ = (7.9 \pm 0.6) \times 10^2$ cm^3 mol^{-1} (333 K), $k_2 = (2.7 \pm 0.3) \times 10^{-4}$ s^{-1} (333 K, 20.0 MPa), $\Delta^\ddagger H_2^\circ = -49 \pm 9$ kJ mol^{-1} (20.0 MPa), $\Delta^\ddagger S_2^\circ = (-4.6 \pm 0.3) \times 10^2$ J mol^{-1} K^{-1} (20.0 MPa), and $\Delta^\ddagger V_2^\circ = (-4.4 \pm 0.6) \times 10^2$ cm^3 mol^{-1} (333 K). In addition, the reaction of H_2tpfpp with $Cu(hfac)_2$ has been studied in *n*-hexane in order to compare the results in $scCO_2$ with those in a conventional nonpolar solvent.

Introduction

Supercritical fluids have been recognized as useful solvents for solvent extraction and liquid chromatography in the field of analytical chemistry, new reaction media for the preparation of new chemical compounds in the field of chemical industry, and unique solvents with wide-range variation in density for the investigation of reaction dynamics in the field of physical chemistry.[1−3] Although many kinds of supercritical fluid are available in a variety of chemical fields, supercritical carbon dioxide ($scCO_2$) is the most widely used because of its innocuous property to the environment and the easiness to produce the supercritical conditions ($T_c = 31.0$ °C, $P_c = 7.3$ MPa). The solubility of many chemical compounds in $scCO_2$ has been measured for the safe separation of toxic materials that infect the environment. Because $scCO_2$ effectively dissolves organic compounds, it has been used as an alternative solvent for extraction to recover them from environmental samples.[4−7] Furthermore, supercritical fluid extraction using an extractant−$scCO_2$ mixture has recently been recognized to have promise as an advanced method for separation of metals from liquid for the purpose of analytical pretreatment or hydrometallurgy.[8,9] Fluorinated *β*-diketones and porphyrins were used as ligands in $scCO_2$ because fluorinated metal complexes possessed excellent solubilities in $scCO_2$.[10] Therefore, quantitative investigation concerning the complexation and substitution reactions of metal ions in $scCO_2$ must be important and required.

To examine the properties of materials dissolved in $scCO_2$, many kinds of instruments have been developed to use in static experiments.[11−22] Some experimental cells have also been developed to follow dynamic change,[23,24] and the kinetics of ligand substitution reactions on metal ions have been investigated in $scCO_2$ for systems containing a photoexcited species.[25−30] To use the $scCO_2$ medium more efficiently, the mechanistic interpretation of the chemical reaction, which is thermally activated in $scCO_2$, is considered to be quite important in addition to the evaluation of the static interaction. However, because of the lack of experimental techniques to follow the change of the reaction system and to determine the reaction rate, such studies in $scCO_2$ and other supercritical fluids are far fewer than the large amount of corresponding studies in

* To whom correspondence should be addressed. E-mail: sfuna@chem4.chem.nagoya-u.ac.jp.
† Research Center for Materials Science.
‡ Graduate School of Science.
§ On leave from the Department of Chemistry, Xiangtan University, China.

10.1021/jp021862k CCC: $25.00
Published on Web 02/15/2003

conventional solvents.[31,32] In this context, we have developed a spectrophotometric cell with a unique circulation system of reactant solution and demonstrated the possibility to determine the reaction rate for slow reactions.[33] Furthermore, because the stopped-flow technique is very useful to start the thermally activated chemical reaction, the stopped-flow instrument ($scCO_2$−SF instrument, Type FIT-7) with spectrophotometric detection, which is applicable for the $scCO_2$ medium,[34] has been newly developed using the know-how of the high-pressure stopped-flow instruments for conventional solvents.[35−39] The $scCO_2$−SF instrument enables us to monitor fast reactions in $scCO_2$ with a half-life longer than ca. 10 ms by rapid mixing of two $scCO_2$ solutions of reactants, which are separately prepared in the $scCO_2$−SF instrument.

In this study, to clarify the metalation mechanism of porphyrins in $scCO_2$, we have investigated the kinetics for the Cu(II) ion incorporation reactions into 5,10,15,20-tetrakis-(pentafluorophenyl)porphyrin (H_2tpfpp) to form the Cu(tpfpp) complex with bis(β-diketonato)copper(II) complexes (CuL_2), such as bis(1,1,1,5,5,5-hexafluoropentane-2,4-dionato)copper-(II) ($Cu(hfac)_2$), bis(1,1,1-trifluoropentane-2,4-dionato)copper-(II) ($Cu(tfac)_2$), bis(2,2,6,6-tetramethylheptane-3,5-dionato)-copper(II) ($Cu(hmac)_2$), and bis(pentane-2,4-dionato)copper(II) ($Cu(acac)_2$) in $scCO_2$ using a newly developed $scCO_2$−SF instrument and spectrophotometric cell. In addition, the solubilities of porphyrin (H_2tpfpp) in $scCO_2$ were measured over a wide range of temperatures (318−378 K) and pressures (10−26 MPa), which were required for the practical measurements of the reaction rate and information on the solute−solvent interaction in $scCO_2$. Furthermore, the metalation rates of H_2tpfpp with $Cu(hfac)_2$ in *n*-hexane were measured in order to compare the reactivity in $scCO_2$ with that in a conventional nonpolar solvent.

Experimental Section

Reagents. H_2tpfpp (Aldrich) and the bis(β-diketonato)copper-(II) complexes (CuL_2), such as $Cu(hfac)_2 \cdot H_2O$ (Aldrich), $Cu(tfac)_2$ (Aldrich), $Cu(hmac)_2$ (Aldrich), and $Cu(acac)_2$ (Wako), were used without further purification. The solvent $scCO_2$ was prepared using liquid carbon dioxide (99.99%, Showa Tansan). *n*-Hexane was dried over activated 4 Å molecular sieves for several days and distilled under a nitrogen atmosphere. The amount of water in *n*-hexane was confirmed to be less than 1×10^{-3} mol kg^{-1} by the Karl−Fisher titration method.

Cu(tpfpp) was prepared by the following procedure. Copper-(II) acetate hydrate (Wako, 54.7 mg, 0.274 mmol) was added to a dimethylformamide (Wako, 30 cm^3) solution of H_2tpfpp (43.9 mg, 0.0450 mmol). The mixture was stirred at 50 °C for 12 h and was then added to 100 cm^3 of water containing NaCl (5 g). The precipitate was collected by filtration and washed well with water. Recrystallization from an ethanol/water mixture gave reddish brown crystals. Anal. calcd for Cu(tpfpp): C, 51.0%; H, 0.8%; N, 5.4%. Found: C, 50.3%; H, 0.8%; N, 5.4%.

UV−Vis Absorption Spectra of Copper(II) Complexes. The UV−vis absorption spectra of $Cu(hfac)_2 \cdot H_2O$, $Cu(tfac)_2$, and $Cu(hmac)_2$ dissolved in $scCO_2$ at 333 K and 20 MPa were recorded using the spectrophotometric measurement system published previously.[33] The absorption peak maxima were observed at 577 and 692, 561 and 687, and 551 and 673 nm for $Cu(hfac)_2 \cdot H_2O$, $Cu(tfac)_2$, and $Cu(hmac)_2$, respectively. The peak maxima of monohydrated $Cu(hfac)_2 \cdot H_2O$ are almost comparable with those of anhydrous $Cu(tfac)_2$ and $Cu(hmac)_2$, indicating that the hydrated water in the $Cu(hfac)_2 \cdot H_2O$ crystal does not bind to the Cu(II) center in $scCO_2$ solution.

Solubility Measurement. The solubility (S) of H_2tpfpp in $scCO_2$ was determined by measuring the UV−vis absorption spectra of the $scCO_2$ solution of H_2tpfpp after the dissolution equilibria of the excess solid samples. The details of the used spectrophotometric cell and the method for the determination of solubility have been previously described.[33] The S values at 313−373 K and 10−30 MPa are listed in Table S1 of the Supporting Information.

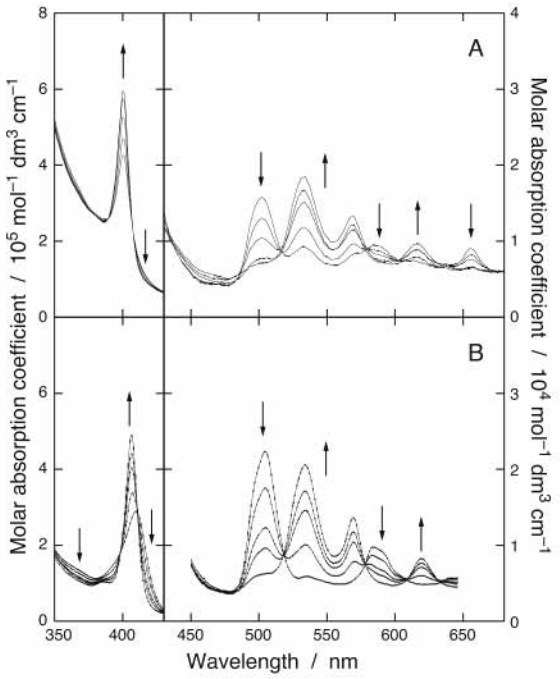

Figure 1. UV−vis absorption spectral change for the reaction between H_2tpfpp and $Cu(hfac)_2$ in $scCO_2$ at 333 K and 20.0 MPa (A) and in *n*-hexane at 308 K and at atmospheric pressure (B). The initial concentrations of $Cu(hfac)_2$ and H_2tpfpp are 1.20×10^{-4} and 1.0×10^{-6} mol dm^{-3} for the left panel in A, 1.00×10^{-3} and 1.0×10^{-5} mol dm^{-3} for the right panel in A, and 5.28×10^{-4} and 3.3×10^{-6} mol dm^{-3} for B, respectively. The absorption spectra at $t = 0.5$, 1, 2, 4, and 8 h (left panel in A), 0.1, 0.3, 0.7, 1.3, and 2.5 h (right panel in A), and 0.03, 2, 6, 10, and 30 h (B) are depicted.

Kinetic Measurements. The measurement procedures of the reaction rates in $scCO_2$ using the spectrophotometric cell and the $scCO_2$−SF instrument were described previously.[33,34] An example of the observed change in the UV−vis absorption spectrum in $scCO_2$ is shown in Figure 1A for the reaction between H_2tpfpp and $Cu(hfac)_2$. The corresponding reactions with the other CuL_2 showed a very similar spectral change. The spectral change was characteristic for the formation of a metalloporphyrin, and the final absorption spectrum of the reaction product was perfectly consistent with that of Cu(tpfpp), which was independently prepared. This indicates that the following reaction takes place.

$$H_2\text{tpfpp} + Cu(hfac)_2 \rightleftarrows Cu(\text{tpfpp}) + 2\text{Hhfac} \qquad (1)$$

All kinetic measurements in $scCO_2$ were carried out under pseudo-first-order conditions where the CuL_2 complex was in a large excess relative to H_2tpfpp. The absorbance (A_λ) change at $\lambda = 401$ nm was found to be first order with respect to H_2tpfpp under the present experimental conditions. The change in A_λ as a function of reaction time (t) was then analyzed according to eq 2

$$A_\lambda = A_\infty - (A_\infty - A_0)\exp(-k_{obs}t) \qquad (2)$$

where A_∞ and A_0 are the absorbances at $t = \infty$ and 0, respectively, and k_{obs} is the conditional first-order rate constant.

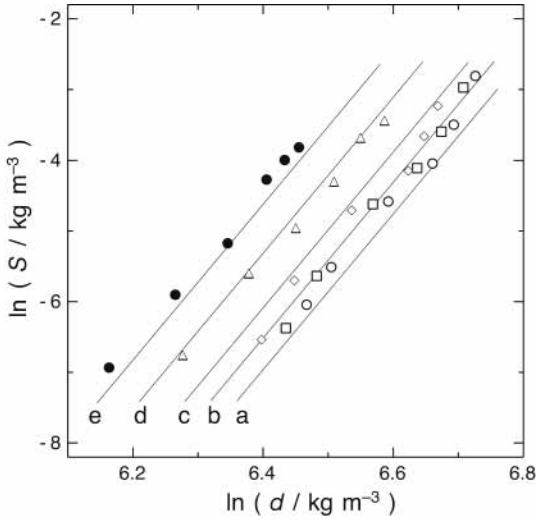

Figure 2. Solubility of H_2tpfpp in $scCO_2$ as a function of density of $scCO_2$ at 313 (a), 323 (b), 333 (c), 353 (d), and 373 K (e). The solid lines represent the calculated values.

The k_{obs} values were determined by varying the total concentration of CuL_2 (C_{Cu}) at various temperatures and pressures, as summarized in Table S2 of the Supporting Information.

The reaction of H_2tpfpp with Cu(hfac)$_2$ in *n*-hexane was followed spectrophotometrically by the conventional mixing method. Figure 1B shows the spectrum change during the reaction. The final spectrum is identical to that of Cu(tpfpp), indicating that the same reaction (eq 1) occurs as that in $scCO_2$. The kinetic measurements in *n*-hexane were performed under pseudo-first-order conditions with an excess concentration of Cu(hfac)$_2$, and the A_{406} value was well-described by eq 2. The k_{obs} values at atmospheric pressure were determined by varying C_{Cu} at 298, 308, 315, and 323 K (Table S3 of the Supporting Information).

Results and Discussion

Solubility of H_2tpfpp. In Figure 2 are plotted the values of ln(S) (kg m^{-3}) as a function of ln(d) (kg m^{-3}), where d is the density of $scCO_2$. The plot at a constant temperature shows almost the linear dependency, and the linear line is monotonically shifted upward with an increase in temperature.

The solubility data were analyzed using the Chrastil's model,[40] which has been adopted for many compounds in $scCO_2$. In the model, the dissolution process of solid H_2tpfpp(s) is divided into the vaporization to form H_2tpfpp(g) and the solvation of H_2tpfpp(g) into $scCO_2$. In $scCO_2$, one molecule of H_2tpfpp is considered to interact with n molecules of CO_2 to form a solvated species of H_2tpfpp·$(CO_2)_n$. The thermodynamics of vaporization are expressed by the Clausius−Clapeyron equation using the heat of vaporization ($\Delta H_v°$) and the corresponding entropy term (q_v). The solvation step can be approximated by the equilibrium constant (K_s) of eq 3

$$H_2\text{tpfpp(g)} + n\text{CO}_2 \overset{K_s}{\rightleftharpoons} H_2\text{tpfpp} \cdot (\text{CO}_2)_n \qquad (3)$$

and the thermodynamic behavior is represented by the reaction heat ($\Delta H_s°$) and the entropy term (q_s). Using the terms of $\Delta H° = \Delta H_v° + \Delta H_s°$ and $q = q_v + q_s$, the solubility (S) in kg m^{-3} is given by eq 4

$$\ln S = n \ln d + \ln\left(\frac{M_p + nM_c}{M_c^{\,n}}\right) - \frac{\Delta H°}{RT} + q \qquad (4)$$

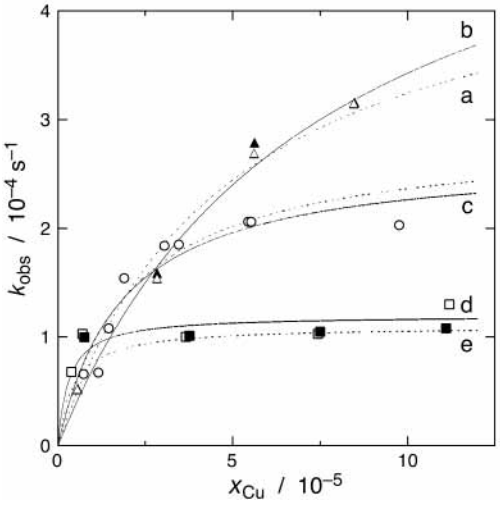

Figure 3. k_{obs} values for the reaction between H_2tpfpp and Cu(hfac)$_2$ in $scCO_2$ as a function of the mole fraction of Cu(hfac)$_2$ at T and P; 323 K and 20.0 MPa (filled triangle), 333 K and 25.0 MPa (open triangle), 333 K and 20.0 MPa (open circle), 333 K and 15.0 MPa (open square), and 353 K and 20.0 MPa (filled square). The solid and broken lines represent the calculated curves for the plot of open and filled markers, respectively.

where d is the density of $scCO_2$ in kg m^{-3}, and M_p and M_c denote the molecular weights of H_2tpfpp and CO_2, respectively. According to the plots in Figure 2, the slopes of the linear function at each temperature were almost constant in the range of 10.8−11.6. Thus, we treated the n value as the constant parameter under the present temperature and pressure conditions. All S data were then analyzed by a least-squares calculation according to eq 4 by optimizing the values of n, $\Delta H°$, and q; the values were obtained as $n = 10.8 \pm 0.4$, $\Delta H° = 37 \pm 3$ kJ mol^{-1}, and $q = -28 \pm 1$. The calculated lines depicted using these parameters represent well the observed solubility data at all temperatures (see Figure 2).

Kinetics for Metalation. In Figure 3, the k_{obs} values for the reaction between H_2tpfpp and Cu(hfac)$_2$ in $scCO_2$ are plotted vs the mole fraction (x_{Cu}) of Cu(hfac)$_2$, which is independent of temperature and pressure. The saturation trend in the k_{obs} values was observed with an increase in x_{Cu}. This dependence indicates that the reaction between H_2tpfpp and Cu(hfac)$_2$ can be expressed by eqs 5 and 6

$$H_2\text{tpfpp} + \text{Cu(hfac)}_2 \overset{K_1}{\rightleftharpoons} H_2\text{tpfpp} \cdot \text{Cu(hfac)}_2 \qquad (5)$$

$$H_2\text{tpfpp} \cdot \text{Cu(hfac)}_2 \xrightarrow{k_2} \text{Cu(tpfpp)} + 2\text{Hhfac} \qquad (6)$$

where K_1 is the equilibrium constant for the fast preequilibrium to form the outer-sphere association complex, H_2tpfpp·Cu(hfac)$_2$, and k_2 is the first-order rate constant of the rate-determining formation of the metalloporphyrin product, Cu(tpfpp). The dissociation of hfac$^-$ from the Cu(II) center prior to the rate determining step can be ruled out, because the k_{obs} values were independent of the added amount of free Hhfac. The k_{obs} values are then expressed by eq 7.[41]

$$k_{obs} = \frac{k_2 K_1 x_{Cu}}{1 + K_1 x_{Cu}} \qquad (7)$$

The k_{obs} values were analyzed by a nonlinear least-squares calculation using eq 7; the optimized values of K_1 and k_2 are summarized in Table 1.

TABLE 1: K_1 and k_2 Values for the Reaction between H_2tpfpp and CuL_2 in $scCO_2$ and *n*-Hexane

CuL_2	T (K)	P (MPa)	d (g cm^{-3})[a]	K_1[b]	k_2 (s^{-1})
			$scCO_2$		
$Cu(hfac)_2$	323	20.0	0.783	1.5×10^4	5.8×10^{-4}
	333	25.0	0.785	1.3×10^4	6.0×10^{-4}
	333	20.0	0.721	5.2×10^4	2.7×10^{-4}
	333	15.0	0.603	4.8×10^5	1.2×10^{-4}
	353	20.0	0.593	2.1×10^6	1.1×10^{-4}
$Cu(tfac)_2$	333	20.0	0.721	2.4×10^5	7.8×10^{-5}
$Cu(hmac)_2$	333	20.0	0.721	2.9×10^6	3.3×10^{-5}
$Cu(acac)_2$	333	20.0	0.721		$\sim 2 \times 10^{-5}$[c]
			n-hexane[d]		
$Cu(hfac)_2$	298	0.1	0.655	2.3×10^2	1.6×10^{-3}
	308	0.1	0.646	4.3×10^2	2.2×10^{-3}
	315	0.1	0.639	6.6×10^2	2.8×10^{-3}
	323	0.1	0.632	1.1×10^3	3.7×10^{-3}

[a] Density of $scCO_2$. [b] Mole fraction unit. [c] Value at $x_{Cu} = 6.17 \times 10^{-6}$. [d] Calculated values using the optimized thermodynamic parameters.

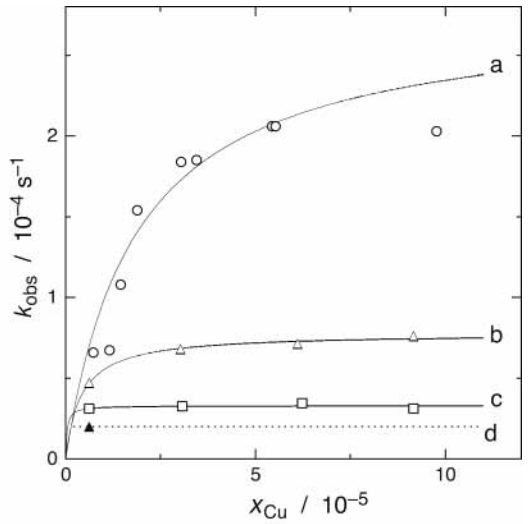

Figure 4. k_{obs} values for the reaction between H_2tpfpp and CuL_2 in $scCO_2$ as a function of the mole fraction of CuL_2 at 333 K and 20.0 MPa for L = hfac (a), tfac (b), hmac (c), and acac (d). The solid line represents the calculated curve.

The k_{obs} values at $T = 333$ K and $P = 20.0$ MPa for the reactions with $Cu(tfac)_2$, $Cu(hmac)_2$, and $Cu(acac)_2$ were plotted vs x_{Cu} in Figure 4 by comparing with those of $Cu(hfac)_2$. The saturating dependence of k_{obs} was also observed for $Cu(tfac)_2$ and $Cu(hmac)_2$, and thus, the values of K_1 and k_2 were determined using eq 7, as given in Table 1. For $Cu(acac)_2$, the k_{obs} value was determined at only one x_{Cu}, because the kinetic experiment for the reaction with $Cu(acac)_2$ was limited by the low solubility of $Cu(acac)_2$ in $scCO_2$.[42]

The temperature dependence of K_1 and k_2 is represented by eq 8 and 9, respectively, at a constant pressure.

$$\ln K_1 = -\frac{\Delta H_1^\circ}{RT} + \frac{\Delta S_1^\circ}{R} \tag{8}$$

$$k_2 = \frac{k_B T}{h} \exp\left(-\frac{\Delta^\ddagger H_2^\circ}{RT} + \frac{\Delta^\ddagger S_2^\circ}{R}\right) \tag{9}$$

where ΔH_1° is the enthalpy change for K_1, ΔS_1° is the corresponding entropy change, R is the gas constant, k_B is the Bolzmann constant, h is the Plank constant, $\Delta^\ddagger H_2^\circ$ is the activation enthalpy for k_2, and $\Delta^\ddagger S_2^\circ$ is the corresponding entropy of activation. By using eqs 7−9, the thermodynamic and kinetic parameters for the reaction between H_2tpfpp and $Cu(hfac)_2$ at 20.0 MPa were optimized by a least-squares calculation. Furthermore, the pressure dependence of K_1 and k_2 at a constant temperature is expressed by eq 10 and 11, respectively.

TABLE 2: Thermodynamic and Kinetic Parameters for K_1 and k_2 for the Reaction between H_2tpfpp and $Cu(hfac)_2$ in $scCO_2$ and *n*-Hexane

parameter	$scCO_2$	*n*-hexane
ΔH_1° (kJ mol^{-1})	76 ± 2[a]	49 ± 3[b]
ΔS_1° (J mol^{-1} K^{-1})	$(3.2 \pm 0.7) \times 10^2$[a]	$(2.1 \pm 0.1) \times 10^2$[b]
ΔV_1° (cm^3 mol^{-1})	$(7.9 \pm 0.6) \times 10^2$[c]	
$\Delta^\ddagger H_2^\circ$ (kJ mol^{-1})	-49 ± 9[a]	25 ± 2[b]
$\Delta^\ddagger S_2^\circ$ (J mol^{-1} K^{-1})	$(-4.6 \pm 0.3) \times 10^2$[a]	$(-2.2 \pm 0.1) \times 10^2$[b]
$\Delta^\ddagger V_2^\circ$ (cm^3 mol^{-1})	$(-4.4 \pm 0.6) \times 10^2$[c]	

[a] At 20.0 MPa. [b] At 0.1 MPa. [c] At 333 K. The values of K_1^0 and k_2^0 are $(1.7 \pm 0.2) \times 10^7$ and $(1.1 \pm 0.4) \times 10^{-5}$ s^{-1}, respectively.

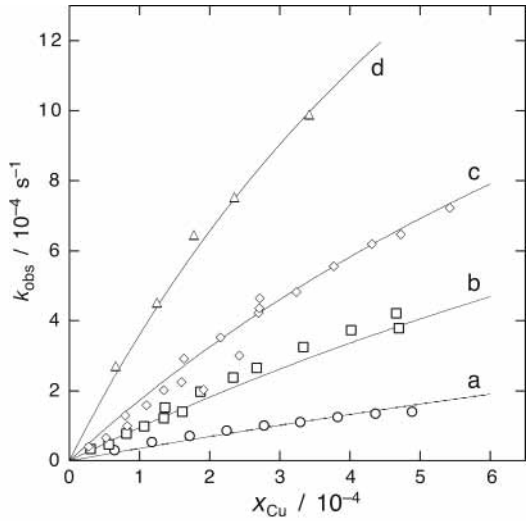

Figure 5. k_{obs} values for the reaction between H_2tpfpp and $Cu(hfac)_2$ in *n*-hexane as a function of the mole fraction of $Cu(hfac)_2$ at 298 (a), 308 (b), 315 (c), and 323 K (d). The solid line represents the calculated curve.

$$\ln K_1 = -\frac{\Delta V_1^\circ}{RT} P + \ln K_1^{\,0} \tag{10}$$

$$\ln k_2 = -\frac{\Delta^\ddagger V_2^\circ}{RT} P + \ln k_2^{\,0} \tag{11}$$

where ΔV_1° is the volume change for K_1, K_1^0 is the K_1 value at $P = 0$, $\Delta^\ddagger V_2^\circ$ is the activation volume for k_2, and k_2^0 is the k_2 value at $P = 0$. The values of ΔV_1°, K_1^0, $\Delta^\ddagger V_2^\circ$, and k_2^0 were optimized by a least-squares calculation using eqs 7, 10, and 11. The obtained thermodynamic and kinetic parameters for the reaction between H_2tpfpp and $Cu(hfac)_2$ are summarized in Table 2.

The k_{obs} values for the reactions with $Cu(hfac)_2$ in *n*-hexane are plotted in Figure 5 as a function of x_{Cu}. The saturating dependence of k_{obs} is seen in Figure 5, although the trend is not very marked. The k_{obs} values are simultaneously analyzed using eqs 7−9 to determine the thermodynamic and kinetic parameters for K_1 and k_2. The optimized parameters at atmospheric pressure are included in Table 2, and the K_1 and k_2 values calculated using those parameters are given in Table 1 at respective measurement temperatures. The calculated curves of k_{obs} vs x_{Cu}

SCHEME 1

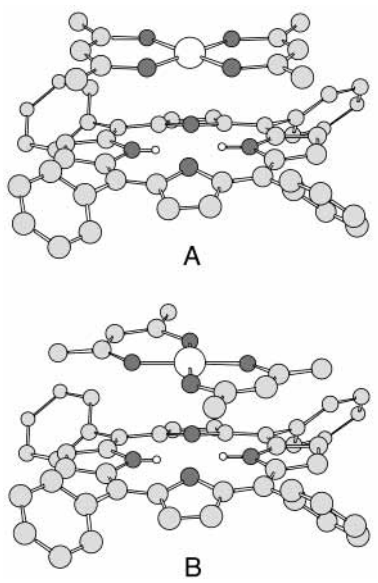

are depicted in Figure 5, and they excellently reproduce the observed k_{obs} values.

Formation of the Outer-Sphere Association Complex in $scCO_2$. As shown in Table 1, the K_1 values are in the order of $Cu(hfac)_2 < Cu(tfac)_2 < Cu(hmac)_2$. This trend is interpreted in terms of both the solvation of the CuL_2 complexes in $scCO_2$ and the electrostatic repulsion between CuL_2 and H_2tpfpp. The solubility of these CuL_2 complexes is reported to be in the order of $Cu(hfac)_2 > Cu(tfac)_2 > Cu(hmac)_2$;[42] that is, the solubility is larger for the CuL_2 complex with the more fluorinated terminal in the β-diketonate ligand. Because the CuL_2 complex with the larger solubility is more stabilized in $scCO_2$, the outer-sphere association between CuL_2 and H_2tpfpp is less advantageous for the CuL_2 complex with the more fluorinated ligand. Furthermore, the electrostatic repulsion between the local negative charges must destabilize the outer-sphere association complex ($H_2tpfpp \cdot CuL_2$). The geometry around the Cu(II) ion in CuL_2 is square planer, and it is not expected that the solvent CO_2 molecules interact at the axial sites of the central Cu(II) ion because of the noncoordinating ability of the CO_2 molecule to the metal ion. Because the porphyrin core of H_2tpfpp also has a planar structure, the H_2tpfpp and CuL_2 molecules may aggregate between their molecular planes in the association complex. In this case, there are two possible forms for the aggregation as shown in Scheme 1, in which the H atoms, except for the pyrrole amine proton, and F atoms are omitted in H_2tpfpp and only the β-diketonato core is depicted in CuL_2 for simplicity. One (Scheme 1A) is the configuration with the four O atoms of CuL_2, which is twisted by 45° from the square composed of the four N atoms of H_2tpfpp. The twist by 45° can avoid efficiently the electrostatic repulsion between the local negative charge on the O atoms of CuL_2 and that on the N atoms of H_2tpfpp. In this configuration, the peripheral pentafluorophenyl groups of H_2tpfpp are closed to the terminal substituents of L of CuL_2; thus, the order in the K_1 value is explained in terms of the electrostatic repulsion between the negatively charged F atoms of H_2tpfpp and CuL_2; that is, the CuL_2 complex with the more fluorinated β-diketonate ligand is less advantageous for the outer-sphere association. The electrostatic repulsion between these terminal groups is diminished in the other configurational possibility (Scheme 1B), in which the four O atoms of CuL_2 are further twisted by 45°. However, in this latter, the negatively charged O atoms of CuL_2 are on top of the negatively charged N atoms of H_2tpfpp. Because the local charge on the O atoms in CuL_2 appears to be more negative for L with the less fluorinated substitution, the electrostatic repulsion between the O and the N atoms anticipated in the configuration of Scheme 1B must be larger for the CuL_2 complex with the more fluorinated L. This latter case will lead to the opposite trend in the K_1 value, and thus, the inconsistency with an experimental finding is considered to support the configuration of Scheme 1A as the association complex formed in the fast preequilibrium step.

The H_2tpfpp and CuL_2 molecules are solvated by CO_2 molecules in $scCO_2$. When the outer-sphere association complex is formed at the K_1 step, the superficies of the association complex will become about a half as compared to the sum of the superficies of both reactants, as expected from the proposed structure (Scheme 1A). The extraordinarily large positive values of $\Delta S_1°$ of 3.2×10^2 J mol^{-1} K^{-1} and $\Delta V_1°$ of 7.9×10^2 cm^3 mol^{-1} are considered to come from the desolvation of the CO_2 molecules accompanied by the outer-sphere association. The finding that the K_1 value is smaller for the more strongly solvated CuL_2 complex also supports the significant contribution of the desolvation of the CO_2 molecules. In addition, the positive value of $\Delta H_1°$ suggests that the deformation of the porphyrin plane is required in the K_1 step in order to interact effectively with the CuL_2 complex. For the most stable planar form of H_2tpfpp, although the pyrrolenine nitrogen atoms are negatively charged, the maximum population of electron density points toward the center of the porphyrin core. The saddle type deformation, in which two pyrrolenine nitrogens are exposed on one side of the porphyrin plane, is considered to be advantageous for the outer-sphere association, and the destruction of the highly conjugated π-system of the porphyrin causes the $\Delta H_1°$ value to be positive.[43] The deformation can also contribute to the large positive values of $\Delta S_1°$ due to the increase in intramolecular freedom in the porphyrin ring.

Rate-Determining Step for Cu(II) Ion Incorporation into Porphyrin in $scCO_2$. According to the recent investigations on the metalation reaction of porphyrins,[44−50] it has been pointed out that the nucleophilic attack of the first pyrrolenine nitrogen on the solvated metal ion is the rate-determining step for the overall metal ion incorporation reaction. Therefore, the nucleophilic attack of the pyrrolenine nitrogen of H_2tpfpp is expected to be included in the rate-determining step. Because the predissociation of L^- from the CuL_2 complex prior to the rate-determining step is experimentally rejected, the pyrrolenine nitrogen is reasonably considered to approach the vacant axial position of the CuL_2 complex. The first-order rate constant k_2 to form the Cu(tpfpp) complex is in the order of $Cu(hfac)_2 > Cu(tfac)_2 > Cu(hmac)_2 > Cu(acac)_2$ (see Table 2); that is, the k_2 value is larger for the CuL_2 complex with the more fluorinated L. This trend is interpreted in terms of (i) the affinity of CuL_2 for the nucleophile of the pyrrolenine nitrogen, (ii) the electrostatic repulsion between H_2tpfpp and CuL_2, and (iii) the Cu−L binding energy. The nucleophilic attack of the pyrrolenine nitrogen is more advantageous for the CuL_2 complex with the more fluorinated L, because more positive charge on the Cu(II) ion is expected for CuL_2 with the less negative O atoms, which is the case of the CuL_2 complex with more fluorinated L. The electrostatic repulsion between the peripheral C_6F_5 groups of H_2tpfpp and the terminal substituents of L contributes to the faster Cu(II) ion incorporation for the CuL_2 complex, since the dissociation of the L^- ligand from the Cu(II) center can be assisted by such repulsion. Furthermore, because the required energy to dissociate L^- from the Cu(II) ion should be smaller

SCHEME 2

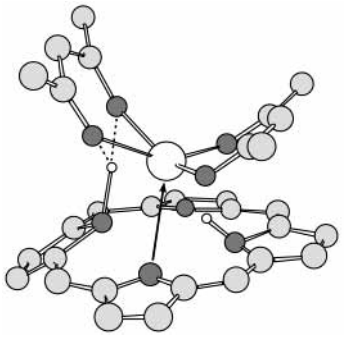

for the CuL_2 complex with the more fluorinated L, as indicated by the stability constants for the formation of CuL_2 in aqueous solution,[51] the activation process is considered to be much easier for the CuL_2 complex with the more fluorinated L. According to the above discussions, an expected feature of the transition state is depicted in Scheme 2.

The most characteristic point for the k_2 value in $scCO_2$ is the decrease with increase in T under a constant P; i.e., the negative value of $\Delta^{\ddagger}H_2^{\circ}$. The negative $\Delta^{\ddagger}H_2^{\circ}$ of -49 kJ mol^{-1}, which corresponds to a large negative solvation enthalpy of activation, suggests that there is a relatively strong interaction and electrostriction at the transition state with localized charge in the outer-sphere association complex due to the elongation of the Cu−O and N−H bonds. The large negative value (-4.6×10^2 J mol^{-1} K^{-1}) of $\Delta^{\ddagger}S_2^{\circ}$ indicates constraint on molecular motion and is consistent with the small $\Delta^{\ddagger}H_2^{\circ}$ due to a highly ordered CO_2 molecule in the transition state. The negative $\Delta^{\ddagger}V_2^{\circ}$ value also implies that the solvation by CO_2 molecules is amplified in the process toward the transition state. The fact that the k_2 value is larger for the CuL_2 complex with the more fluorinated L, which is dissociated easier from the Cu(II) ion, supports that the Cu−O bond is elongated during the activation process. The elongation should lead to the charge separation between the Cu(II) ion and the dissociating L^- ligand, and the CO_2 molecule is considered to be constrained by the generated charge. This means that the solvation exceeds the increment in volume due to elongation of the bonds. Furthermore, the pyrrole amine proton of H_2tpfpp should be attracted by the dissociating L^- ligand, and it is also possible that the generating partial negative charge in the conjugated π-system of H_2tpfpp caused by the abstraction of the proton contributes to enhancing the solvation by CO_2 molecules.

Metalation of H_2tpfpp with Cu(hfac)$_2$ in *n*-Hexane. As indicated above, the reaction process for the metalation of H_2tpfpp with Cu(hfac)$_2$ in *n*-hexane is the same as in $scCO_2$, which is expressed by eqs 5 and 6 with K_1 for the fast preequilibrium of the outer-sphere association and k_2 for the rate-determining formation of the metalloporphyrin. Here, let us compare the thermodynamic and kinetic parameters for K_1 and k_2 in $scCO_2$ and *n*-hexane under the present experimental conditions, which are summarized in Table 2. The finding that the K_1 value in $scCO_2$ is much larger than that in *n*-hexane is reflected in the extraordinarily large positive value of ΔS_1°, which comes from the desolvation of the CO_2 molecules accompanied by the outer-sphere association. The k_2 value in *n*-hexane is by 1 order of magnitude larger than that in $scCO_2$. This metalation rate is strongly affected by the entropy factor. Especially, the $\Delta^{\ddagger}S_2^{\circ}$ value in $scCO_2$ is found to be much more negative at -4.6×10^2 J mol^{-1} K^{-1}, which is twice relative to that in *n*-hexane. Interestingly, it is worthwhile pointing out that the $\Delta^{\ddagger}H_2^{\circ}$ value in *n*-hexane is positive but negative in $scCO_2$. This negative $\Delta^{\ddagger}H_2^{\circ}$ indicates a large negative solvation enthalpy of activation reflecting the electrostriction around the transition state with localized charge due to elongation of the Cu−O and N−H bonds. This implies that the enthalpy for solvation exceeds the exothermic enthalpy due to the elongation of the bonds. The ΔV_1° value in $scCO_2$ is very much larger 7.9×10^2 cm^3 mol^{-1}, corresponding to a large positive ΔS_1°. The $\Delta^{\ddagger}V_2^{\circ}$ in $scCO_2$ has a very much larger negative value (-4.4×10^2 cm^3 mol^{-1}), corresponding to a large negative $\Delta^{\ddagger}S_2^{\circ}$. Thus, the pressure effect on K_1 and k_2 in $scCO_2$ is drastically greater as compared with that in a conventional solvent such as *n*-hexane.

Conclusions

Copper(II) ion incorporation into fluorinated porphyrin (H_2tpfpp) to form the metalloporphyrin (Cu(tpfpp)) has been kinetically investigated with bis(β-diketonato)copper(II) complexes (CuL_2) in $scCO_2$ and *n*-hexane. The reaction mechanism seems to be identical in both solvents. The copper(II) ion incorporation reaction proceeds via two steps: the fast outer-sphere association between H_2tpfpp and CuL_2 prior to the rate-determining step and the rate-determining copper(II) ion incorporation into the porphyrin core. The outer-sphere association complex has the configuration with the four O atoms of CuL_2, which is twisted by 45° from the square composed of the four N atoms of H_2tpfpp. Thus, the CuL_2 complex with the more fluorinated β-diketonate ligand is less advantageous for the association; that is, the K_1 values are in the order of Cu(hfac)$_2$ < Cu(tfac)$_2$ < Cu(hmac)$_2$. During the activation processes, the first pyrrolenine nitrogen of H_2tpfpp in the outer-sphere association complex will nucleophilically approach the vacant axial position of the CuL_2 complex, and at the same moment, the elongation of the Cu−O bond in CuL_2 and the N−H bond in H_2tpfpp occurs concertedly by electrostatic interaction (see Scheme 2). The fact that the k_2 values are in the order of Cu(hfac)$_2$ > Cu(tfac)$_2$ > Cu(hmac)$_2$ > Cu(acac)$_2$ may be explained by the affinity of CuL_2 for the nucleophile of the pyrrolenine nitrogen, the ease of dissociation of the β-diketonate ligand, and the electrostatic repulsion between H_2tpfpp and CuL_2 in the transition state. The most characteristic feature in $scCO_2$ relative to *n*-hexane is the desolvation and solvation effects, which are reflected, respectively, in the largely positive ΔS_1° and ΔV_1° values obtained for K_1 and the largely negative $\Delta^{\ddagger}S_2^{\circ}$ and $\Delta^{\ddagger}V_2^{\circ}$ values obtained for k_2.

Acknowledgment. This work was supported by Grants-in-Aid for Scientific research (Nos. 11354009, 11554030, and 12874094) from the Ministry of Education, Science, Sports and Culture of Japan and the REIMEI Research Resources of Japan Atomic Energy Research Institute. A grant from the Japan Society for the Promotion of Science for S.L. is gratefully acknowledged.

Supporting Information Available: The results of the solubility of H_2tpfpp in $scCO_2$ (Table S1), the k_{obs} values for the reaction between H_2tpfpp and CuL_2 in $scCO_2$ (Table S2), and the k_{obs} values for the reaction between H_2tpfpp and Cu(hfac)$_2$ in *n*-hexane (Table S3). This material is available free of charge via the Internet at http://pubs.acs.org.

References and Notes

(1) Kiran, E., Brennecke, J. F., Eds. *Supercritical Fluid Engineering Science: Fundamentals and Applications*; American Chemical Society: Washington, DC, 1993.

(2) Kiran, E., Debenedetti, P. G., Peters, C. J., Eds. *Supercritical Fluids: Fundamentals and Applications*; Kluwer Academic Publishers: Dordrecht, 1998.

(3) Clifford, T. *Fundamentals of Supercritical Fluids*; Oxford University Press: Oxford, 1999.
(4) Smith, R. M., Ed. *Supercritical Fluid Chromatography*; The Royal Society of Chemistry: Cambridge, 1993.
(5) de Castro, M. D. L.; Valcárcel, M.; Tena, M. T. *Analytical Supercritical Fluid Extraction*; Springer-Verlag: New York, 1994.
(6) Taylor, L. T. *Supercritical Fluid Extraction*; John Wiley & Sons: New York, 1996.
(7) Chester, T. L.; Pinkston, J. D. *Anal. Chem.* **2000**, *72*, 129R.
(8) Dehghani, F.; Wells, T.; Cotton, N. J.; Foster, N. R. *J. Supercrit. Fluids* **1996**, *9*, 263.
(9) Wu, H.; Lin, Y.; Smart, N. G.; Wai, C. M. *Anal. Chem.* **1996**, *68*, 4072.
(10) Darr, J. R.; Poliakoff, M. *Chem. Rev.* **1999**, *99*, 495.
(11) Yokoyama, C.; Kanno, Y.; Takahashi, M.; Ohtake, K.; Takahashi, S. *Rev. Sci. Instrum.* **1993**, *64*, 1369.
(12) Hansen, B. N.; Lagalante, A. F.; Sievers, R. E.; Bruno, T. J. *Rev. Sci. Instrum.* **1994**, *65*, 2112.
(13) Murata, T.; Nakagawa, K.; Kimura, A.; Otoda, N.; Shimoyama, I. *Rev. Sci. Instrum.* **1995**, *66*, 1437.
(14) Kojima, J.; Nakayama, Y.; Takenaka, M.; Hashimoto, T. *Rev. Sci. Instrum.* **1995**, *66*, 4066.
(15) Kazarian, S. G.; Vincent, M. F.; Eckert, C. A. *Rev. Sci. Instrum.* **1996**, *67*, 1586.
(16) Wallen, S. L.; Pfund, D. M.; Fulton, J. L.; Yonker, C. R.; Newville, M.; Ma, Y. *Rev. Sci. Instrum.* **1996**, *67*, 2843.
(17) Hoffmann, M. H.; Conradi, M. S. *Rev. Sci. Instrum.* **1997**, *68*, 159.
(18) Dukes, K. E.; Harbron, E. J.; Forbes, M. D. E.; DeSimone, J. M. *Rev. Sci. Instrum.* **1997**, *68*, 2505.
(19) Jwayyed, A. M.; Humayun, R.; Tomasko, D. L. *Rev. Sci. Instrum.* **1997**, *68*, 4542.
(20) Kirby, C. F.; McHugh, M. A. *Rev. Sci. Instrum.* **1997**, *68*, 3150.
(21) Addleman, R. S.; Hills, J. W.; Wai, C. M. *Rev. Sci. Instrum.* **1998**, *69*, 3127.
(22) Hourri, A.; St-Arnaud, J. M.; Bose, T. K. *Rev. Sci. Instrum.* **1998**, *69*, 2732.
(23) Zhang, J.; Connery, K. A.; Strebinger, R. B.; Brennecke, J. F.; Chateauneuf, J. E. *Rev. Sci. Instrum.* **1995**, *66*, 3555.
(24) Ji, Q.; Eyring, M.; van Eldik, R.; Reddy, K. B.; Goates, S. R.; Lee, M. L. *Rev. Sci. Instrum.* **1995**, *66*, 222.
(25) Ji, Q.; Eyring, E. M.; van Eldik, R.; Johnston, K. P.; Goates, S. R.; Lee, M. L. *J. Phys. Chem.* **1995**, *99*, 13461.
(26) Banister, J. A.; Cooper, A. I.; Howdle, S. M.; Jobling, M.; Poliakoff, M. *Organometallics* **1996**, *15*, 1804.
(27) Sun, X.-Z.; George, M. W.; Kazarian, S. G.; Nikiforov, S. M.; Poliakoff, M. *J. Am. Chem. Soc.* **1996**, *118*, 10525.
(28) Ji, Q.; Lloyd, C. R.; Eyring, E. M.; van Eldik, R. *J. Phys. Chem. A* **1997**, *101*, 243.
(29) Sun, X.-Z.; Grills, D. C.; Nikiforov, S. M.; Poliakoff, M.; George, M. W. *J. Am. Chem. Soc.* **1997**, *119*, 7521.
(30) Grills, D. C.; Sun, X.-Z.; Childs, G. I.; George, M. W. *J. Phys. Chem. A* **2000**, *104*, 4300.
(31) Lee, P. D.; King, J. L.; Seebald, S.; Paliakoff, M. *Organometallics* **1998**, *17*, 524.
(32) Linehan, J. C.; Yonker, C. R.; Bays, J. T.; Autrey, S. T. *J. Am. Chem. Soc.* **1998**, *120*, 5826.
(33) Sato, H.; Inada, Y.; Nagamura, T.; Funahashi, S. *J. Supercrit. Fluids* **2001**, *21*, 71.
(34) Inada, Y.; Sato, H.; Horita, T.; Nagamura, T.; Funahashi, S. *J. Supercrit. Fluids* **2001**, *21*, 205.
(35) Funahashi, S.; Ishihara, K.; Tanaka, M. *Inorg. Chem.* **1981**, *20*, 51.
(36) Ishihara, K.; Funahashi, S.; Tanaka, M. *Rev. Sci. Instrum.* **1982**, *53*, 1231.
(37) Funahashi, S.; Ishihara, K.; Inamo, M.; Tanaka, M. *Inorg. Chim. Acta* **1989**, *157*, 65.
(38) Ishihara, K.; Miura, H.; Funahashi, S.; Tanaka, M. *Inorg. Chem.* **1988**, *27*, 1706.
(39) Funahashi, S.; Ishihara, K.; Aizawa, S.; Sugata, T.; Ishii, M.; Inada, Y.; Tanaka, M. *Rev. Sci. Instrum.* **1993**, *64*, 130.
(40) Chrastil, J. *J. Phys. Chem.* **1982**, *86*, 3016.
(41) Wilkins, R. G. *The Study of Kinetics and Mechanism of Reactions of Transition Metal Complexes*; Allyn and Bacon: Boston, 1974. As pointed out on page 28 in ref 41, the same kinetic behavior as in eq 7 was obtained if the complex was viewed as a "dead end" intermediate in rapid equilibrium and if the reaction proceeded bimolecularly between H_2tpfpp and Cu(hfac)$_2$. Steady state kinetics alone will not distinguish between these two mechanisms; arguments over which of the two is preferred must then be based on the chemical or rate considerations. As discussed later, the mechanism expressed by eq 7 followed by reactions 5 and 6 must be plausible. A related subject has been reported. Takeda, J.; Ohya, T.; Sato, M. *Inorg. Chem.* **1992**, *31*, 2877.
(42) Lagalante, A. F.; Hasen, B. N.; Bruno, T. J.; Sievers, R. E. *Inorg. Chem.* **1995**, *34*, 5781.
(43) Cheng, B.; Munro, O. Q.; Marques, H. M.; Scheidt, W. R. *J. Am. Chem. Soc.* **1997**, *119*, 10732.
(44) Inada, Y.; Sugimoto, Y.; Nakano, Y.; Funahashi, S. *Chem. Lett.* **1996**, 881.
(45) Nakano, Y.; Sugimoto, Y.; Inada, Y.; Funahashi, S. *J. Inorg. Biochem.* **1997**, *67*, 124.
(46) Inada, Y.; Sugimoto, Y.; Nakano, Y.; Itoh, Y.; Funahashi, S. *Inorg. Chem.* **1998**, *37*, 5519.
(47) Inada, Y.; Nakano, Y.; Inamo, M.; Nomura, M.; Funahashi, S. *Inorg. Chem.* **2000**, *39*, 4793.
(48) Inada, Y.; Yamaguchi, T.; Satoh, H.; Funahashi, S. *Inorg. Reac. Mech.* **2000**, *2*, 277.
(49) Funahashi, S.; Inada, Y.; Inamo, M. *Anal. Sci.* **2001**, *17*, 917.
(50) Inamo, M.; Kamiya, N.; Inada, Y.; Nomura, M.; Funahashi, S. *Inorg. Chem.* **2001**, *40*, 5636.
(51) Sekine, T.; Ihara, N. *Bull. Chem. Soc. Jpn.* **1971**, *44*, 2942.